International Journal of Mass Spectrometry 280 (2009) 113–118

Contents lists available at ScienceDirect

International Journal of Mass Spectrometry

journal homepage: www.elsevier.com/locate/ijms

Isomer-specific product detection of CN radical reactions with ethene and propene by tunable VUV photoionization mass spectrometry

Adam J. Trevitt[a], Fabien Goulay[b], Giovanni Meloni[b], David L. Osborn[b], Craig A. Taatjes[b], Stephen R. Leone[a,*]

[a] Departments of Chemistry and Physics and Lawrence Berkeley National Laboratory, University of California, Berkeley, CA 94720, USA
[b] Combustion Research Facility, Mail Stop 9055, Sandia National Laboratories, Livermore, CA 94551-0969, USA

ARTICLE INFO

Article history:
Received 1 June 2008
Received in revised form 26 July 2008
Accepted 30 July 2008
Available online 8 August 2008

Keywords:
Product detection
CN radical
Alkenes
Synchrotron
Titan

ABSTRACT

Product detection studies of CN reactions with ethene and propene are conducted at room temperature (4 Torr, 533.3 Pa) using multiplexed time-resolved mass spectrometry with tunable synchrotron photoionization. Photoionization efficiency curves, i.e., the ion signal as a function of photon energy, are used to determine the products and distinguish isomers. Both reactions proceed predominantly via CN addition to the π orbital of the olefin. For CN + ethene, cyanoethene (C_2H_3CN) is detected as the sole product in agreement with recent studies on this reaction. Multiple products are identified for the CN + propene reaction with 75(±15)% of the detected products in the form of cyanoethene from a CH_3 elimination channel and 25(±15)% forming different isomers of C_4H_5N via H elimination. The C_4H_5N comprises 57(±15)% 1-cyanopropene, 43(±15)% 2-cyanopropene and <15% 3-cyanopropene. No evidence of direct H abstraction or indirect HCN formation is detected for either reaction. The results have relevance to the molecular weight growth chemistry on Saturn's largest moon Titan, where the formation of small unsaturated nitriles are proposed to be key steps in the early chemical stages of haze formation.

1. Introduction

The CN radical is present in diverse chemical environments including flames [1], comets [2], extraterrestrial atmospheres (in particular Saturn's largest moon, Titan) and interstellar molecular clouds [3]. Above the haze in the Titanian atmosphere CN can be generated from the photolysis of HCN. The subsequent CN reactions with olefins, including ethene and propene, can lead to unsaturated nitriles. Nitrile-forming reactions are key components in the molecular weight growth chemistry of haze formation [4–6]. Rate coefficients for CN reactions with small olefins have been determined over a wide range of temperatures in numerous kinetic studies [7–10]. At low temperatures (<300 K) these reactions generally proceed via barrierless entrance channels with rate constants typically on the order of 10^{-10} cm^3 molecule^{-1} s^{-1}. Experimental product detection studies on the other hand are more scarce. In crossed beam experiments, Balucani et al. have investigated a range of CN reactions with unsaturated hydrocarbons [11,12], including ethene. The CN + ethene reaction was observed to produce cyanoethene (C_2H_3CN) via H elimination. The formation of HCN + C_2H_3 from either direct H abstraction or indirect HCN elimination could not be probed in the Balucani et al. study. A subsequent computational Rice–Ramsperger–Kassel–Marcus (RRKM) study of CN + ethene by Vereecken et al. [13] reported C_2H_3CN + H as the dominant product channel (>90%) at pressures below 10^4 Pa at 300 K. The HCN + C_2H_3 product channel was found to contribute less than 5% under these conditions and stabilization of radical intermediate adduct complexes are only significant at pressures greater than 10^6 Pa.

In a recent study, Gannon et al. reported H atom product yields for CN reactions with ethene and propene by monitoring the production of H atoms using Lyman-α laser-induced atomic fluorescence [14]. At 298 K, close to unity H atom product yield was measured for CN + ethene but in the case of CN + propene, a yield of 0.478 (±0.045) at 2 Torr was reported. A RRKM-master equation analysis on the CN + propene potential energy surface was fitted to the experimental data in order to predict product branching fractions, including the H, CH_3 and HCN elimination channels. Indirect HCN elimination and direct H abstraction were not found to be significant pathways. Since this study was only capable of detecting H atoms there was no direct experimental verification of the branching fractions to other possible products or isomers. More comprehensive product detection experiments, where all major

* Corresponding author. Tel.: +1 510 643 5467; fax: +1 510 643 1376.
E-mail address: srl@berkeley.edu (S.R. Leone).

1387-3806/$ – see front matter © 2008 Elsevier B.V. All rights reserved.
doi:10.1016/j.ijms.2008.07.033

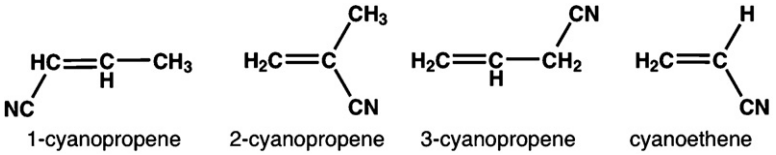

Fig. 1. Nitrile products relevant in this study.

products are detected in quantifiable amounts, are desirable in order to identify all the significant product pathways.

In this paper we investigate the CN reactions with ethene and propene using tunable vacuum ultraviolet (VUV) synchrotron photoionization coupled with time-resolved multiplexed mass spectrometry. This technique enables the detection of all the major product channels simultaneously and the identification of specific product isomers. Fig. 1 depicts the structures of the C_4H_5N product isomers and cyanoethene (C_2H_3CN) relevant to this undertaking. The following reaction channels are considered in this study (thermochemical data from Refs. [15,16]):

$$\begin{aligned} CN(X^2\Sigma^+) + C_2H_4 &\rightarrow C_2H_3 + HCN \quad (-53\,kJ/mol) \\ &\rightarrow C_2H_3CN + H \quad (-96\,kJ/mol) \end{aligned}$$

$$\begin{aligned} CN(X^2\Sigma^+) + C_3H_6 &\rightarrow \textit{trans}\text{-1-cyanopropene} + H \quad (-140\,kJ/mol) \\ &\rightarrow \textit{cis}\text{-1-cyanopropene} + H \quad (-134\,kJ/mol) \\ &\rightarrow \text{2-cyanopropene} + H \quad (-107\,kJ/mol) \\ &\rightarrow \text{3-cyanopropene} + H \quad (-157\,kJ/mol) \\ &\rightarrow C_2H_3CN + CH_3 \quad (-136\,kJ/mol) \\ &\rightarrow C_3H_5 + HCN \quad (-149\,kJ/mol) \end{aligned}$$

For CN + ethene we show that the one product channel producing cyanoethene (C_2H_3CN) is dominant. In the case of CN + propene multiple product masses are detected, corresponding to H and CH_3 elimination. Analysis of photoionization efficiency (PIE) curves, where the ion signal for a product is plotted as a function of photon energy, reveals 1-cyanopropene and 2-cyanopropene as the products of the H elimination channel and cyanoethene as the sole coproduct formed with CH_3 elimination. With approximations for the photoionization cross-section, estimates of product branching ratios to all the major product channels are obtained. These results have interesting implications for Titan, since the formation of nitriles, particularly cyanoethene (C_2H_3CN), are implicated in the early stages of haze formation.

2. Experimental methods

2.1. Instrumentation

The apparatus used in this work is essentially the same as described in several previous studies [17–19]. The experimental configuration, depicted schematically in Fig. 2, comprises a slow-flow reaction tube interfaced to a multiplexed photoionization mass spectrometer. This configuration is inspired by the design of Slagle and Gutman [20]. The flow reactor is a 600 mm long quartz tube with a 10.5 mm inner diameter. Calibrated mass flow controllers deliver the radical precursor (ICN vapor, 1.86×10^{13} cm^{-3}), the reactant (propene, 3.9×10^{13} cm^{-3} or ethene, 6.5×10^{14} cm^{-3}) and He buffer gas (1.3×10^{17} cm^{-3}). The room temperature gas mixture migrates through the flow tube towards a vacuum pump via a feedback-regulated throttle valve that maintains the 4 Torr (533.3 Pa) gas pressure used in all the experiments reported here. Flow rates are typically around 4 m/s and are sufficient to replenish the gas in time for the next laser photolysis pulse.

The radical-neutral chemistry in the gas flow is initiated by an unfocussed, 20 ns pulse of 248 nm laser radiation from a KrF excimer laser that generates CN radicals ($\sim 2 \times 10^{12}$ cm^{-3}) from ICN photolysis uniformly down the gas column at a 4 Hz repetition rate. Typical laser fluences are 20 mJ/cm^2. Photolysis of ICN at 248 nm gives rise to CN radicals primarily in the vibrational ground state [14,21], and any rotational excitation will be quickly equilibrated by collisions. A 650 μm pinhole, located 350 mm downstream from the flow tube entrance, allows a small quantity of gas to escape into a surrounding chamber pumped by a 3200 L s^{-1} turbo pump. This nearly effusive gas beam, containing reactants, reaction products and He bath gas, is skimmed by a 1.5 mm diameter skimmer as it enters the differentially pumped ionization region. At this point the gas beam is intersected by synchrotron undulator radiation that has been dispersed by a 3 m monochromator at the Chemical Dynamics Beamline of the Advanced Light Source (ALS). A gas cell containing Ar at 30 Torr (4 kPa) is positioned after the synchrotron undulator to absorb higher-order undulator harmonics. The quasi-continous VUV synchrotron radiation ionizes molecular species that arrive in the ionization region. These ions are subsequently accelerated, focussed and dispersed by a double-focussing magnetic sector mass spectrometer (Mattauch–Herzog configuration) [22], and the ions impact upon a position-sensitive microchannel plate detector with a delay-line anode [23]. With this configuration each ion is distinguished by its mass-to-charge ratio and tagged with a time of arrival relative to the pulsing of the excimer laser. The experiment is repeated for 400 laser pulses at each synchrotron photon energy, typically achieving signal-to-noise levels >100. In this paper, where emphasis is not so much on kinetics but on product detection, the data are binned at 500 μs time intervals unless stated otherwise.

By scanning the photon energy of the synchrotron radiation, time resolved mass spectra are recorded over a desired range of photonionization energies, resulting in a three-dimensional data matrix consisting of ion intensity as a function of ion mass-to-charge (m/z), photoionization energy and reaction time. The photon energy resolution used in this study was 40 meV and was calibrated by measurement of the atomic resonances of Xe and the sharp autoionization resonances of oxygen. The ion signals are background corrected by averaging the signal 20 ms prior to the photolysis laser pulse and subtracting this from the post-laser signal for the same m/z channel. All data obtained as a function of photon energy are normalized for changes in the ALS photon flux.

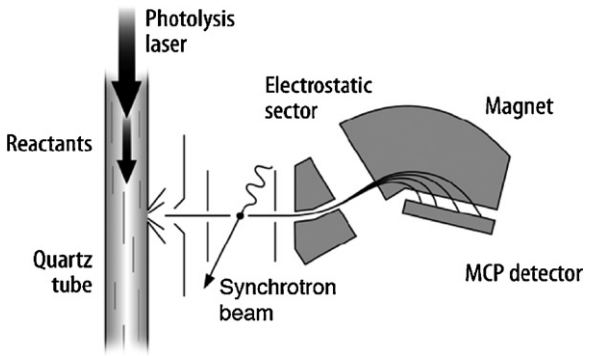

Fig. 2. Schematic diagram of the experiment.

2.2. Computational methods

The overall shape and onset of the PIE curves are simulated within the Franck–Condon (FC) approximation, using calculated molecular geometries and force constants. Electronic structure calculations of the neutral product species and their cations are carried out using the Gaussian03 package [24] The composite method CBS-QB3 [25,26] is utilized to obtain optimized bond distances, harmonic vibrational frequencies, and force constants together with reliable energetics [26]. All the vibrational frequencies are real, indicating that the optimized geometries represent minima in the potential energy surface. The simulated FC PIE curves are obtained by computation and integration of the photoelectron spectra at a temperature of 300 K, using the PESCAL program [27,28] within the Franck–Condon approximation including Duschinsky rotation [29]. The fits are shifted (typically <20 meV), well within the energy resolution of the measurement, to match the onsets of the experimentally determined PIE curves.

3. Results and discussion

3.1. CN + ethene

The CN + ethene mass spectrum acquired at 11.05 eV photon energy is shown in Fig. 3a. One product peak is observed at $m/z = 53$, consistent with the $C_3H_3N + H$ product channel. The temporal evolution of the $m/z = 53$ ion signal (Fig. 3b) reveals that the ion count rises abruptly after the photolysis laser pulse (0 ms) and remains essentially constant over the duration of the measurement, suggesting that the detected product is an unreactive, closed-shell species. Considering the ethene concentration (6.5×10^{14} cm^{-3}) and the known rate coefficient for the CN + ethene reaction (2.5×10^{-10} cm^3 molecule^{-1} s^{-1} at 298 K [21]) the timscale of the reaction is on the order of 10 μs. This fast kinetics results in an instantaneous rise of the signal within the experimental temporal resolution. Identification of this C_3H_3N species is achieved by integrating the ion signal from 0 ms to 80 ms as a function of photon energy. The result is a PIE curve shown in Fig. 3c. The likely isomer at this mass is cyanoethene (CH_2CHCN) [11,13], which has an adiabatic ionization energy (AIE) of 10.91 eV [30] in agreement with the ion signal onset present in Fig. 3c. Our calculated AIE of 10.90 eV for cyanoethene matches very well with the experimental value. Pathways to other C_3H_3N isomers are energetically unfavorable [11,13]. The He(I) photoelectron (PE) spectrum of cyanoethene has been previously recorded [30]. The PE spectrum integrated over energy is shown along with the measured PIE curve in Fig. 3c. There is good agreement with both the signal onset and the ion signal trend versus photon energy, confirming cyanoethene as the major reaction product.

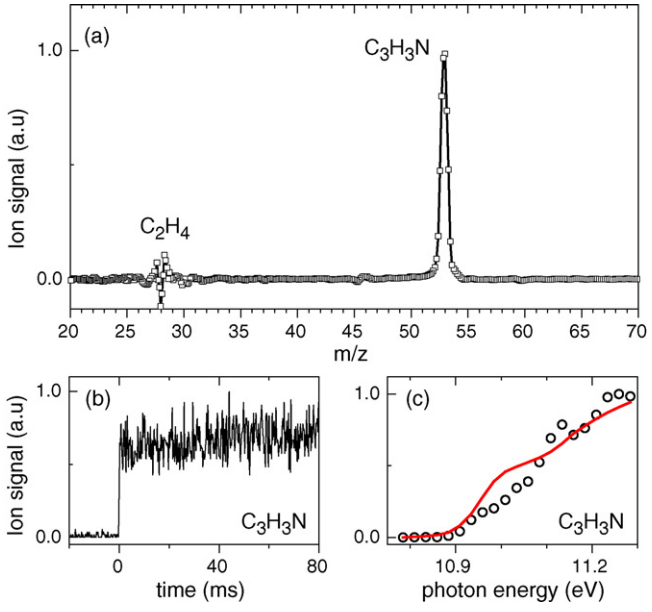

Fig. 3. (a) Mass spectrum of the CN + ethene reaction (11.05 eV), (b) time profile of the $m/z = 53$ peak (the photolysis laser is pulsed at 0 ms) and (c) photoionization efficiency plot of the ion signal $m/z = 53$ as a function of synchrotron photon energy (circles) and integrated PE spectrum from Ref. [30] (line).

A CN + ethene mass spectrum was also acquired at 10.1 eV (not shown), below the AIE of ethene (10.51 eV [31]) but well above the known AIE of the vinyl radical C_2H_3 (8.25 eV [32]), to check for the C_2H_3+HCN product channel. Only a few ion counts were detectable at $m/z = 27$ (C_2H_3) after a significant integration period, suggesting that this product channel is very weak (<2% using a 11 Mb[1] cross-section at 10.1 eV [33]). Indeed, close to unity H atom product yields have been measured for the CN + ethene reaction [14,21] and RRKM calculations predict the $HCN + C_2H_3$ channel to contribute <5% at these conditions [13]. Direct detection of HCN in the current experimental configuration is difficult due to the high ionization energy of HCN (>13.6 eV), which is substantially higher than the AIEs of the reactants and major products. At these high-photon energies dissociative ionization of the major product species can produce HCN, rendering it difficult to distinguish HCN generated from reaction channels. It is a possibility that vinyl radicals are produced but react rapidly before reaching the detector. The likely co-reactants in high concentration are ethene and ICN. The vinyl + ethene reaction is slow (6.0×10^{16} cm^3 molecule^{-1} s^{-1} at 298 K [34]). No data are available for the ICN + vinyl reaction but radical reactions with ICN tend to be relatively slow. The energy resolved mass spectra do not contain any products that would indicate reactions of the vinyl radical are occurring.

The likely reaction pathway for CN + ethene starts with CN addition on the π-orbital of ethene forming the CH_2CH_2CN radical. From the CH_2CH_2CN radical intermediate there are two competing pathways, direct H elimination to CH_2CHCN and a 1,2 H-shift forming CH_3CHCN. The CH_3CHCN intermediate subsequently decomposes to also form $CH_2CHCN + H$. Computational RRKM studies predict that, of the CH_2CHCN formed, 60% originates from the CH_3CHCN intermediate and 40% directly from the CH_2CH_2CN intermediate [11,13]. Given that both pathways form $CH_2CHCN + H$, the present study draws no conclusions regarding these competing mechanisms.

An interesting possibility for CN reactions is the formation of iso-cyano adducts (–NC). For CN + ethene Vereecken et al. in constructing a potential energy surface and performing a RRKM analysis, find that the rate of formation of the CH_2CH_2CN intermediate, which is the more exoergic addition channel, dominates over CH_2CH_2NC. Furthermore, the transition state to the $CH_2CHNC + H$ product channel from the –NC intermediate is an unfavorable +12 kJ/mol relative to the reactants [13]. Our CBS-QB3 calculations predict that the AIE of isocyanoethylene (CH_2CHNC) is 10.56 eV, well below the measured ion signal onset. Balucani et al. conclude that C_2H_3NC was not observed in their crossed beam studies [11]. Fig. 3c shows good agreement between the measured PIE and the literature curve for cyanoethene (–CN adduct) and, together with the calculated AIE of isocyanoethene, our results are in accord with these previous studies that concluded the –NC adduct complex

[1] 1 Mb (megabarn) = 10^{-18} cm^2.

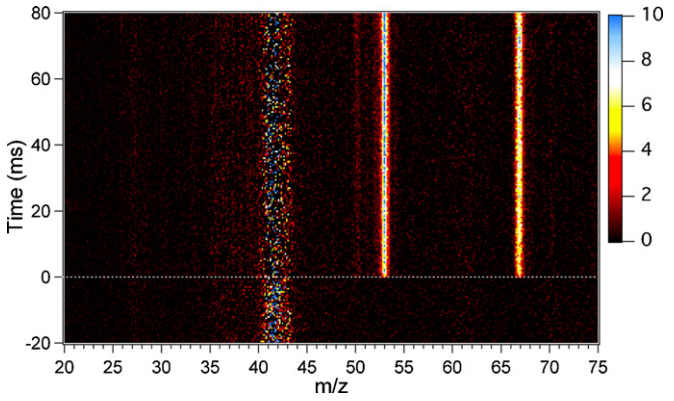

Fig. 4. Time resolved mass spectrum of the CN + propene reaction integrated from 9.6 eV to 11.5 eV. The photolysis laser occurs at 0 ms (dashed line).

does not contribute to any product species. The formation of HNC via direct abstraction is also unlikely due to a calculated 56 kJ/mol barrier [13].

3.2. CN + propene

Fig. 4 shows a time-resolved mass spectrum of the CN + propene reaction that has been integrated over a range of photon energies (9.6–11.5 eV). Two product masses are apparent at $m/z = 53$ and $m/z = 67$, which appear immediately after the photolysis laser is pulsed and remain constant over the 80 ms measurement. Again, this sharp rise time is consistent with the literature rate coefficient for the CN + propene reaction (2.4×10^{-10} cm^3 molecule^{-1} s^{-1} at 298 K [8]). The detected masses correspond to reaction products of the form C_3H_3N (53 amu) from CH_3 elimination and C_4H_5N (67 amu) from H elimination. To identify the products present in Fig. 4, PIE curves were measured by recording the ion signal as a function of the photon energy. The PIE curve for $m/z = 53$ is shown in Fig. 5. At this mass there is only one plausible product, cyanoethene resulting from CN addition onto propene and subsequent CH_3 elimination. As before, the He(I) photoelectron spectrum of cyanoethene [30] has been integrated over energy and shown in Fig. 5. There is very good agreement between the recorded PIE curve and the integrated PE spectrum of cyanoethene. A slight difference is noted in the slopes of the cyanoethene PIE curves from the CN + ethene and CN + propene experiments and is attributed to experimental variations. The reproducible feature at 11.1 eV in both curves is possibly due to an auto-ionizing resonance.

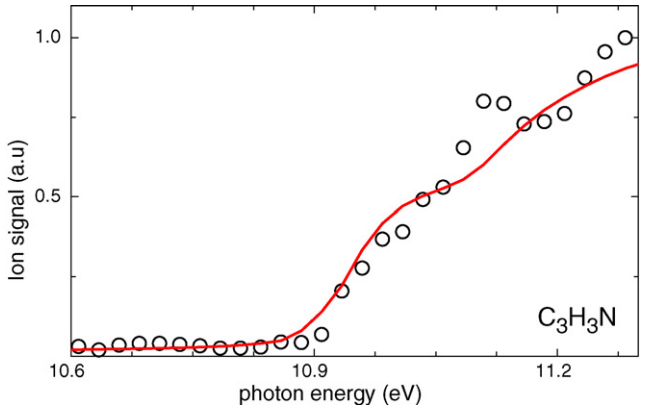

Fig. 5. Photoionization efficiency curve of $m/z = 53$ product signal from the CN + propene reaction (circles) and the integrated PE spectrum of cyanoethene taken from Ref. [30] (line).

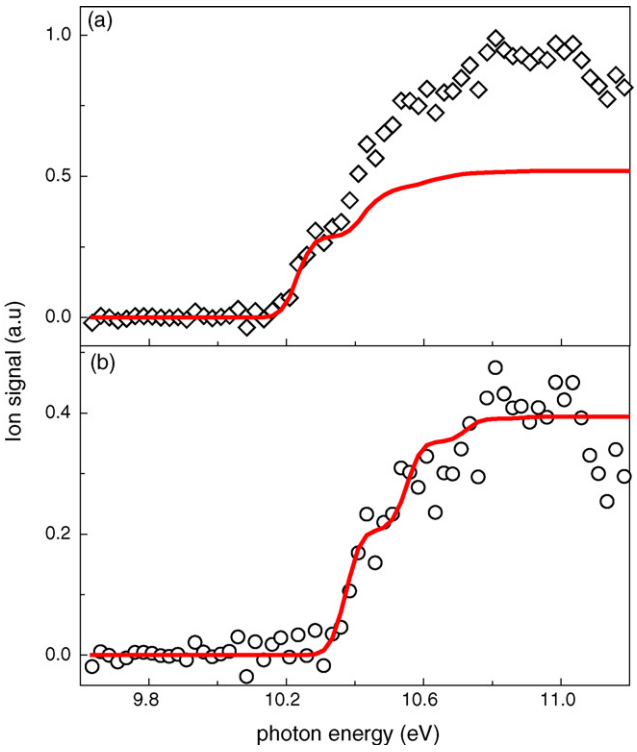

Fig. 6. (a) The photoionization efficiency plot of $m/z = 67$ product signal from the CN + propene reaction and the fitted contribution of 1-cyanopropene (line) and (b) the remainder $m/z = 67$ product signal after the fitted contribution of 1-cyanopropene has been subtracted and the fitted contribution of 2-cyanopropene (line).

Fig. 6a is a PIE curve for $m/z = 67$ that reveals a sharp onset of signal at 10.22 eV. At this mass, resulting from H atom elimination, the likely products of the molecular formula C_4H_5N are 1-cyanopropene, 2-cyanopropene and 3-cyanopropene (shown in Fig. 1). Both 2-cyanopropene and 3-cyanopropene have been investigated by threshold photoelectron photoion coincidence [35] and conventional photoelectron [30,36] spectroscopies and thus their AIEs are known. The AIE of 2-cyanopropene is 10.34 eV. The AIE of 3-cyanopropene appears to be at 10.18 eV but is comparatively weak in reported photoelectron spectra, with the strongest transition within the first vibronic band appearing at 10.60 eV. [35,36]. These Franck-Condon factors result in a rather slow-rising onset in the 3-cyanopropene PIE curve, at odds with the sharp rise in Fig. 6a. The third plausible product, 1-cyanopropene, to our knowledge does not have a reported PIE or PE spectrum but a vertical ionization potential of 10.23 ± 0.05 eV has been reported in a photoelectron study [37]. The PIE curve of 1-cyanopropene was simulated based on the calculated ionization energy and Franck–Condon factors. Since 1-cyanopropene has trans and cis conformations, PIE curves for both stereoisomers were simulated and the adiabatic ionization energies were found to be 10.21 eV and 10.23 eV, respectively, having similar Franck–Condon envelopes. At the resolution of the experiment (40 meV) the two are essentially indistinguishable and the cis conformation was used in the analysis. We rule out the presence of 1-isocyanopropene based on its calculated AIE of 10.03 eV. A good fit exists between the data points of the signal onset ~10.20 eV and the onset of the simulated PIE curve for 1-cyanopropene (shown in Fig. 6a). The second step in the PIE curve at ~10.35 eV corresponds well to the known AIE of 2-cyanopropene (10.34 eV) suggesting that these two isomers contribute to the PIE curve. To determine the relative contributions of these three isomers, photoionization cross-section values are required. However,

these data are not available in the literature so approximations for the photoionization cross-sections were made by implementing a semi-emperical method reported by Bobeldijk et al. [38] based on summing the contributions of atom pairs. Using this method, 1-cyanopropene, 2-cyanopropene and 3-cyanopropene have, to within 20%, a photoionization cross-section of 20 Mb at 11.8 eV, and all PIE curves were normalized to this value. A least squares fitting routine was executed to determine the weighted contributions of the three isomers between 10.10 eV and 11.06 eV. The best fit was found to correspond to 57(±15)% 1-cyanopropene and 43(±15)% 2-cyanopropene where the errors are reported as 2σ incorporating the uncertainties in both the fit and the photoionization cross-sections. Fig. 6b shows the experimental PIE data after the fitted contribution for 1-cyanopropene has been subtracted and is plotted along with the fitted portion of the simulated 2-cyanoproprene PIE. Up to 11.06 eV, all the experimental data points are well reproduced by the fitted combination of these two isomers. The contribution of the 3-cyanopropene PIE (from the PE spectrum extracted from Ref. [30]) was zero in the best fit. Within the limits of certainty, the 3-cyanopropene isomer contributes <15% to the C_4H_5N PIE. At higher photon energies (>11.06 eV) the depletion in the experimental ion signal is probably due to dissociative ionization from 1-cyanopropene since the appearance energies of fragment ions from 2-cyanopropene are >11.65 eV [35].

Fig. 7 is a mass spectrum of the CN + propene reaction integrated from 0 ms to 80 ms, summed over 2000 photolysis laser pulses, at 11.04 eV photoionization energy. The two product peaks corresponding to C_2H_3CN (m/z = 53) and C_4H_5N (m/z = 67) are evident. The feature at m/z = 42 represents a small residual signal from reactant propene that was not completely removed by the background subtraction method. The peaks corresponding to C_2H_3CN and C_4H_5N have an integrated peak area ratio of 1.00:0.70 in favor of C_2H_3CN (m/z = 53). No pressure dependence for this ratio was observed over the pressure interval of 1–6 Torr. Photoionization cross-section estimates at 11.04 eV, for C_2H_3CN and the C_4H_5N isomers, were determined by first approximating the photoionization cross-sections at 11.8 eV, using the aforementioned semi-emperical method of Bobeldijk et al. [38], and then normalizing the simulated PIE curves to this value. For the C_4H_5N species, the photoionization cross-section value at 11.04 eV is approximately the same as 11.8 eV, that is 20 ± 4 Mb. In the case of cyanoethene a cross-section of 14 ± 3 Mb is approximated at 11.8 eV and, based on the simulated PIE curve, the cross-section at 11.04 eV is expected to be ∼60% of this value, which equates to 9 ± 3 Mb. None of the species under consideration have transitions near 11.8 eV in photoelectron spectra [30,35,37] nor in the simulated Franck–Condon envelopes that would add further uncertainty to the photoionization cross-section approximations. Correcting for the respective photoionization cross-sections provides a ratio of C_2H_3CN to C_4H_5N product formation of 0.75 ± 0.15 (CH_3 loss) to 0.25 ± 0.15 (H loss), with the stated errors incorporating the uncertainties in the photoionization cross-section approximations and the measurement. Altogether, in this study of the detected products of the CN + propene reaction the branching fractions are 75(±15)% cyanoethene + CH_3, and 25(±15)% to the C_4H_5N + H channel with the C_4H_5N signal found to comprise 57(±15)% 1-cyanopropene, 43(±15)% 2-cyanopropene and <15% 3-cyanopropene. We checked for the presence of a signal at m/z = 41 (allyl radical, C_3H_5), produced from direct H abstraction by CN or a HCN elimination mechanism by acquiring a mass spectrum at 9.68 eV photon energy, below the AIE of propene (9.73 eV [39]) but above the AIE of allyl (8.13 eV [40]). No signal at m/z = 41 was detected. Reactive collisions, involving allyl with propene or ICN, are expected to be relatively slow and should not inhibit allyl detection. We assign an upper limit to this channel of 2% considering an allyl photoionization cross-section of 6 Mb [41]. Using the Vereecken et al. [13] CN + ethene as a guide, the stabilization of radical intermediate species in the CN + propene reaction is not expected to be significant at the pressures used in this study (<10 Torr). Nor do we observe any mass spectrometric evidence for any radical intermediates.

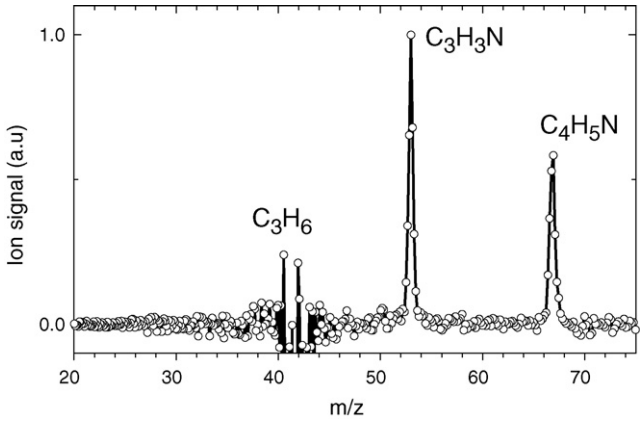

Fig. 7. Mass spectrum of the CN + propene reaction at 11.04 eV.

From measured H atom yields for the CN + propene reaction, Gannon et al. [14] report H atom branching fractions of 0.392 ± 0.050 at 5 Torr and 0.478 ± 0.045 and 2 Torr. Interpolating linearly to 4 Torr yields 0.420 ± 0.050. This branching fraction to H + C_4H_5N is significantly greater than the branching fraction derived in the present work of 0.25 ± 0.15 by measuring both the co-product signals from both the H elimination (C_4H_4N) and CH_3 elimination (C_2H_3CN) channels. Another point of difference relates to the pressure dependence of the H atom yield. As mentioned above, we find that in measuring both product channels simultaneously the ratio of the C_2H_3CN and C_4H_5N signals at 11.04 eV remained constant over 1–6 Torr (within 5% with no systematic trend).

The potential energy surface of the CN + propene reaction constructed by Gannon et al. [14] reveals that two intermediates are likely after barrierless CN addition: a primary radical ($CH_3CH(CN)CH_2$) and a 10 kJ/mol lower energy secondary radical (CH_3CHCH_2CN). They report that the primary radical intermediate almost entirely leads to the formation of cyanoethene + CH_3 (92%) with the remainder forming 2-cyanopropene + H. In the case of the secondary radical intermediate the significant exit channels are a 1,2 H shift yielding cyanoethene + CH_3 and the direct H elimination forming 1-cyanopropene. The competing exit channels from the secondary radical intermediate, H elimination and the 1,2 H shift, are shown to proceed via transition state barriers calculated to differ by only 3 kJ/mol. Within this framework, the H atom yield predominantly depends first on the relative populations of the primary and secondary radical intermediates and then, in turn, the competition between the H elimination (forming 1-cyanopropene) and CH_3 elimination from the secondary radical. By fitting experimental H atom yield data to a RRKM-master equation analysis, Gannon et al. find 80% secondary radical intermediate formation and 20% for the primary radical intermediate and product yields of 0.51 cyanoethene + CH_3, 0.47 1-cyanopropene + H and 0.02 2-cyanopropene + H. Assessing these predictions in comparison to the findings of the current study, both 2-cyanopropene + H and cyanoethene + CH_3 are in greater yield in our experiments. This result suggests that the 20% yield assigned to the primary radical intermediate from the RRKM-master equation fit may be too low. There may also exist other significant pathways not considered in the RRKM master-equation analysis that feed the 2-cyanopropene and

cyanoethene exit channels. The small energy difference (3 kJ/mol) calculated between the transition states for the competing H elimination and 1,2 H shift pathways from the secondary radical intermediate might also be a point of uncertainty that could strongly influence predicted branching ratios. We note that the highest level electronic structure calculations for transition state energies in molecules of this size typically have uncertainties of at least ±4 kJ/mol.

The results of this product detection study have implications for the chemistry of Titan's atmosphere. In the upper Titanian atmosphere, it is proposed that the nitrile contribution to haze formation is largely due to [6]:

$$CN + C_2H_3CN \rightarrow \text{polymer} \quad (1)$$

The CN reactions with ethene and propene are kinetically rapid at temperatures applicable to Titan's atmosphere (~100 K) [8] and, as shown in the current study, both reactions yield large fractions of C_2H_3CN (cyanoethene). It therefore seems plausible that both these reactions are important in the early stages of molecular weight growth chemistry leading to haze formation particularly in the upper atmosphere where significant quantities of C_2H_3CN have been detected by the ion neutral mass spectrometer (INMS) on the *Cassini* spacecraft [42].

4. Conclusion

Using synchrotron radiation coupled with time-resolved multiplexed mass spectrometry, we have investigated the reaction of CN with ethene and propene. Both reactions proceed via CN addition to the olefin. For ethene, the only product detected was cyanoethene (CH_2CHCN) consistent with CN addition and H elimination. In the case of the CN + propene reaction, the following products were detected and assigned branching fractions: cyanoethene (CH_2CHCN) 75(±0.15)% and 25(±0.15)% C_4H_5N. The C_4H_5N signal is found to comprise of 57(±15)% 1-cyanopropene, 43(±15)% 2-cyanopropene and <15% 3-cyanopropene. No evidence for direct H abstraction or HCN elimination was detected in either the CN + ethene or propene reactions.

Acknowledgements

SRL thanks Zdenek Herman for his exquisite insights and delightful interactions with the flowing afterglow ion group on his extended visits to Boulder, CO.

We thank Mr. Howard Johnsen for his excellent technical assistance. The support of personnel (A.J.T.) for this research by the National Aeronautics and Space Administration (Grant NAGS-13339) is gratefully acknowledged. Sandia authors and the instrumentation for this work are supported by the Division of Chemical Sciences, Geosciences, and Biosciences, the Office of Basic Energy Sciences, the U.S. Department of Energy. Sandia is a multiprogram laboratory operated by Sandia Corporation, a Lockheed Martin Company, for the National Nuclear Security Administration under contract DE-AC04-94-AL85000. The Advanced Light Source and Chemical Sciences Division (S.R.L.) are supported by the Director, Office of Science, Office of Basic Energy Sciences of the U.S. Department of Energy under Contract No. DE-AC02-05CH11231 at Lawrence Berkeley National Laboratory.

References

[1] J. Luque, J.B. Jeffries, G.P. Smith, D.R. Crosley, Combust. Flame 126 (2001) 1725.
[2] N. Fray, Y. Bénilan, H. Cottin, M.-C. Gazeau, J. Croviser, Planet. Space Sci. 53 (2005) 1243.
[3] A. Rodrguez-Franco, J. Martin-Pinato, A. Fuente, Astron. Astrophys. 329 (1998) 1097.
[4] E.H. Wilson, S.K. Atreya, Planet. Space Sci. 51 (2003) 1017.
[5] J.H. Waite Jr., D.T. Young, T.E. Cravens, A.J. Coates, F.J. Crary, B. Magee, J. Westlake, Science 316 (2007) 870.
[6] P.P. Lavvas, A. Coustenis, I.M. Vardavas, Planet. Space Sci. 56 (2008) 27.
[7] L. Herbert, I.W.M. Smith, R.D. Spencer-Smith, Int. J. Chem. Kinet. 24 (1992) 791.
[8] I.R. Sims, J.-L. Queffelec, D. Travers, B.R. Rowe, L.B. Herbert, J. Karthauser, I.W.M. Smith, Chem. Phys. Lett. 211 (1993) 461.
[9] M.T. Butterfield, T. Yu, M.C. Lin, Chem. Phys. 169 (1993) 129.
[10] S.W. North, R. Fei, T.J. Sears, G.E. Hall, Int. J. Chem. Kinet. 27 (1997) 129.
[11] N. Balucani, O. Asvany, A.H.H. Chang, S.H. Lin, Y.T. Lee, R.I. Kaiser, Y. Osamura, J. Chem. Phys. 113 (2000) 8643.
[12] N. Balucani, O. Asvany, A.H.H. Chang, S.H. Lin, Y.T. Lee, R.I. Kaiser, Y. Osamura, H.F. Bettinger, Astrophys. J. 545 (2000) 892.
[13] L. Vereecken, P.D. Groof, J. Peeters, Phys. Chem. Chem. Phys. 5 (2003) 5070.
[14] K.L. Gannon, D.R. Glowacki, M.A. Blitz, K.J. Hughes, M.J. Pilling, P.W. Seakins, J. Phys. Chem. A 111 (2007) 6679.
[15] P.J. Linstrom, W.G. Mallard (Eds.), NIST Chemistry WebBook, Standard Reference Database Number 69, National Institute of Standards and Technology, Gaithersburg, MD, June 2005, p. 20899 (http://webbook.nist.gov).
[16] S.G. Lias, J.E. Bartmess, J.F. Liebman, J.L. Holmes, R.D. Levin, W.G. Mallard, J. Phys. Chem. Ref. Data 17 (Suppl. 1) (1988).
[17] G. Meloni, P. Zou, S.J. Klippenstein, M. Ahmed, S.R. Leone, C.A. Taatjes, D.L. Osborn, J. Am. Chem. Soc. 128 (2006) 14310.
[18] F. Goulay, D.L. Osborn, C.A. Taatjes, P. Zou, G. Meloni, S.R. Leone, Phys. Chem. Chem. Phys. 9 (2007) 4291.
[19] G. Meloni, T.M. Selby, F. Goulay, S.R. Leone, D.L. Osborn, C.A. Taatjes, J. Am. Chem. Soc. 129 (2007) 14025.
[20] I.R. Slagle, D. Gutman, J. Am. Chem. Soc. 107 (1985) 5342.
[21] N. Choi, M.A. Blitz, K. McKee, M.J. Pilling, P.W. Seakins, Chem. Phys. Lett. 384 (2004) 68.
[22] M.P. Sinha, M. Wadsworth, Rev. Sci. Instrum. 76 (2005) 025103.
[23] J.V. Vallerga, W.O.H. Siegmund, Nucl. Instrum. Methods Phys. Res. A 442 (2000) 159.
[24] M.J. Frisch, G.W. Trucks, H.B. Schlegel, G.E. Scuseria, M.A. Robb, J.R. Cheeseman, J.J.A. Montgomery, K.N.K.T. Vreven, J.C. Burant, J.M. Millam, S.S. Iyengar, J. Tomasi, V. Barone, B. Mennucci, M. Cossi, G. Scalmani, N. Rega, G.A. Petersson, H. Nakatsuji, M. Hada, M. Ehara, K. Toyota, R. Fukuda, J. Hasegawa, M. Ishida, T. Nakajima, Y. Honda, O. Kitao, H. Nakai, M. Klene, X. Li, J.E. Knox, H.P. Hratchian, J.B. Cross, V. Bakken, C. Adamo, J. Jaramillo, R. Gomperts, R.E. Stratmann, O. Yazyev, A.J. Austin, R. Cammi, C. Pomelli, J.W. Ochterski, P.Y. Ayala, K. Morokuma, G.A. Voth, P. Salvador, J.J. Dannenberg, V.G. Zakrzewski, S. Dapprich, A.D. Daniels, M.C. Strain, O. Farkas, D.K. Malick, A.D. Rabuck, K. Raghavachari, J.B. Foresman, J.V. Ortiz, Q. Cui, A.G. Baboul, S. Clifford, J. Cioslowski, B.B. Stefanov, G. Liu, A. Liashenko, P. Piskorz, I. Komaromi, R.L. Martin, D.J. Fox, T. Keith, M.A. Al-Laham, C.Y. Peng, A. Nanayakkara, M. Challacombe, P.M.W. Gill, B. Johnson, W. Chen, M.W. Wong, C. Gonzalez, J.A. Pople, Gaussian03, Gaussian, Inc., Wallingford, CT, 2004.
[25] J.A. Montgomery, M.J. Frisch, J.W. Ochterski, G.A. Petersson, J. Chem. Phys. 110 (1999) 2822.
[26] J.A. Montgomery, M.J. Frisch, J.W. Ochterski, G.A. Petersson, J. Chem. Phys. 112 (2000) 6532.
[27] K.M. Ervin, T.M. Ramond, G.E. Davico, R.L. Schwartz, S.M. Casey, W.C. Lineberger, J. Phys. Chem. A 105 (2001) 10822.
[28] K.M. Ervin, PESCAL, Fortran Program, University of Nevada, Reno, 2004.
[29] F. Duschinsky, Acta Physicochim. URSS 7 (1937) 551.
[30] K. Ohno, S. Matsumoto, K. Imai, Y. Harada, J. Phys. Chem. 88 (1984) 206.
[31] B.A. Williams, T.A. Cool, J. Chem. Phys. 94 (1991) 6358.
[32] J.A. Blush, P. Chen, J. Phys. Chem. A 96 (1992) 4138.
[33] J.C. Robinson, N.E. Sveum, D.M. Neumark, J. Chem. Phys. 119 (2003) 5311.
[34] H. Ismail, C.F. Goldsmith, P.R. Abel, P.-T. Howe, A. Fahr, J.B. Halpern, L.E. Jusinski, Y. Georgievskii, C.A. Taatjes, W.H. Green, J. Phys. Chem. A 111 (2007) 6843.
[35] G.D. Willet, T. Baer, J. Am. Chem. Soc. 102 (1980) 6664.
[36] R.F. Lake, H.T. Thompson, Proc. Roy. Soc., Lond. A 317 (1970) 187.
[37] K.N. Houk, L.L. Munchausen, J. Am. Chem. Soc. 98 (1976) 937.
[38] M. Bobeldijk, W.J. van der Zande, P.G. Kistemaker, Chem. Phys. 179 (1994) 125.
[39] J.C. Traeger, Int. J. Mass Spectrom. Ion. Proc. 58 (1984) 259.
[40] F.A. Houle, J.L. Beauchamp, J. Am. Chem. Soc. 100 (1978) 3291.
[41] J.C. Robinson, N.E. Sveum, D.M. Neumark, Chem. Phys. Lett. 383 (2004) 601.
[42] V. Vuitton, R.V. Yelle, V.G. Anicich, APJ 647 (2006) L175.